Ray-tracing and eikonal solutions for low-frequency wavefields

Chad M. Hogan and Gary F. Margrave

ABSTRACT

High-frequency approximations to the wavefield, such as the eikonal equation and ray-tracing, are only valid when the scale of variation in the medium is significantly larger than the wavelengths considered. Geology, however, commonly varies on spatial scales that are comparable to or even smaller than the typical wavelengths used in seismic imaging. We investigate the possible consequences of this effect, and test one simple method for extending the range of validity of eikonal and ray-tracers: a frequency-dependent Gaussian smoothing of the underlying velocity model.

We show that this smoothing not only leads to eikonal and ray-tracing solutions which better match the kinematics of the full wavefield, but also leads to a convergence of eikonal and ray-tracing solutions. Although there are other methods for treating band-limited ray-paths, the primary advantage of this method is its simplicity.

INTRODUCTION

Many migration algorithms rely on a high-frequency approximation to simplify calculations. One of the most common is the separation of a wave equation into eikonal and transport equations. This allows the approximate solution of the wave equation via two separate steps: first, the solution of the traveltime from source and receiver to a given subsurface location, and second, these traveltimes are used to derive the approximate amplitudes of the wavefield at these points.

Previous work (Hogan and Margrave, 2006) has shown that GPSPI (Margrave and Ferguson, 1999) and related imaging algorithms can benefit from a frequency-dependent smoothing of the underlying velocity model. Therefore, it seems natural to test whether or not standard eikonal and ray-tracing techniques can benefit from smoothing. Other methods of treating band-limited data exist (e.g. Woodward, 1992, and references therein), but the primary advantage of this method is its simplicity.

Beginning with a derivation of the eikonal and transport equations, the frequency-dependence of this approximation will be shown. Following this, a demonstration of the frequency-dependent mismatch of the eikonal solution wavefront with full finite-difference solutions will given, and then a frequency-dependent smoothing will be shown to improve the match.

THE EIKONAL EQUATION

This treatment follows one given by Pujol (2003). To derive the eikonal equation, begin with a scalar wave equation with position coordinate $\vec{x}$ and time t,

$$\left(\nabla^2 - \frac{1}{v^2(\vec{x})}\partial_t^2\right)\Psi(\vec{x},t) = 0. \tag{1}$$

Fourier transform $t \rightarrow \omega$:

$$\nabla^2 \psi(\vec{x}, \omega) = \frac{\omega^2}{v^2(\vec{x})} \psi(\vec{x}, \omega). \tag{2}$$

Now assume a solution of form:

$$\psi(\vec{x}, \omega) = A(\vec{x}, \omega) e^{i\omega\phi(\vec{x})}. \tag{3}$$

Now we calculate the component of the ∇^2 operator for each spatial axis j,

$$\partial_j^2 \psi = \left(\partial_j^2 A + 2iA + iA\omega \partial_j^2 \phi - A\omega^2 \left(\partial_j \phi \right)^2 \right) e^{i\omega\phi}. \tag{4}$$

Using trial solutions from equation 3, combining with equation 4, substituting into equation 2, cancelling the exponential, dividing by $A\omega^2$, and rearranging yields

$$\left((\partial_j \phi)^2 - \frac{1}{v^2} \right) - \frac{i}{\omega} \left(\frac{2}{A} \partial_j A \partial_j \phi + \partial_j^2 \phi \right) - \frac{1}{\omega^2 A} \partial_j^2 A = 0. \tag{5}$$

This solution can be simplified by noting that in the limit as $\omega \rightarrow \infty$ the first term in equation 5 dominates. This leads to the *eikonal equation*,

$$|\nabla \phi(\vec{x})|^2 = \frac{1}{v^2(\vec{x})}. \tag{6}$$

This equation is fundamentally valid only in this limit. This implies that the eikonal equation (and many other ray-tracing techniques) may only be used when variations in velocity are negligible on spatial scales that are comparable to the wavelengths of the propagating waves. Since seismic data typically contains useful frequencies in the range 5 – 100 Hz over media varying between 1500 – 6000 m/s, this implies a wavelength range of at least 15 – 1200 m. This in turn implies that this "high frequency" approximation will be valid when the medium variability is only on scales of hundreds of meters or larger.

The *transport equation* is derived by considering only the second term in equation 5, setting it equal to zero, and multiplying by $2A\omega/i$:

$$2\nabla A \cdot \nabla \phi + A \nabla^2 \phi = 0 \tag{7}$$

The hypereikonal equation

We will define reference slowness $S_0(\vec{x})$ such that

$$S_0^2(\vec{x}) = \frac{1}{v^2(\vec{x})} = |\nabla \phi(\vec{x})|^2. \tag{8}$$

By inserting this into the full-dimensional version of equation 5 and considering only the real part, we arrive at the *hypereikonal* or *frequency-dependent eikonal* equation,

$$\left| \nabla \tilde{\phi}(\vec{x}, \omega) \right|^2 = S^2(\vec{x}, \omega) = S_0(\vec{x})^2 + \frac{1}{\omega^2} \frac{\nabla^2 A(\vec{x}, \omega)}{A(\vec{x}, \omega)}. \tag{9}$$

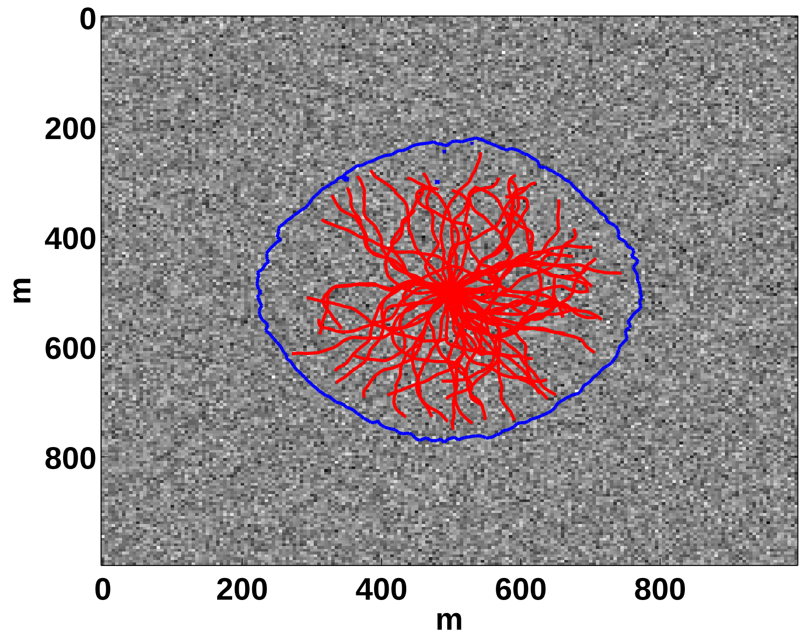

FIG. 1. Ray tracing (in red) through a $2000m/s, \sigma = 500m/s$ medium. The eikonal solution envelope for the same propagation time is overlaid in blue.

This reference slowness is the "natural" slowness model of the medium, while this new slowness $S(\vec{x}, \omega)$ is a frequency-dependent effective slowness. We have also extended ϕ as defined in equation 3 to depend upon both ω and $\vec{x}$.

This hypereikonal equation allows a solution of frequency-dependent traveltimes through a medium. Reference slowness S_0 is used to find traveltimes for the limiting case $\omega \rightarrow \infty$, while the frequency-dependent slownesses give traveltimes for finite frequencies. Note that the only assumption made in this hypereikonal equation is that solutions of the form given in equation 3 may be found – this is not another high frequency approximation.

Biondi (1997) has shown that it is feasible to solve numerically for these frequency-dependent slownesses, with some moderate linearization in the equation. The solutions reveal a sort of frequency-dependent smoothing, with heavy smoothing at low frequencies, and very little smoothing at high frequencies. This smoothing allows ray-tracing that matches propagation front very well with full-wavefield solutions. Unfortunately, these solutions are somewhat complicated to calculate accurately and in a stable fashion.

The physics of the eikonal equation

Physically, the eikonal equation may be thought of as defining an outer envelope which would approximately contain all rays traced from the start time $t = 0$ to the travel time t. Consider a medium consisting of a homogeneous background velocity of 2000 m/s but with random fluctuations of a nearly-normal distribution with a standard deviation of 500 m/s but with velocities outside of 2σ set to 2σ. In Figure 1, ray tracing through this medium is shown, along with the eikonal solution for the same propagation time. Note how very few of the rays actually approach the traveltime given by the eikonal solution. If this medium is lightly smoothed, the rays much more readily agree with the eikonal solution,

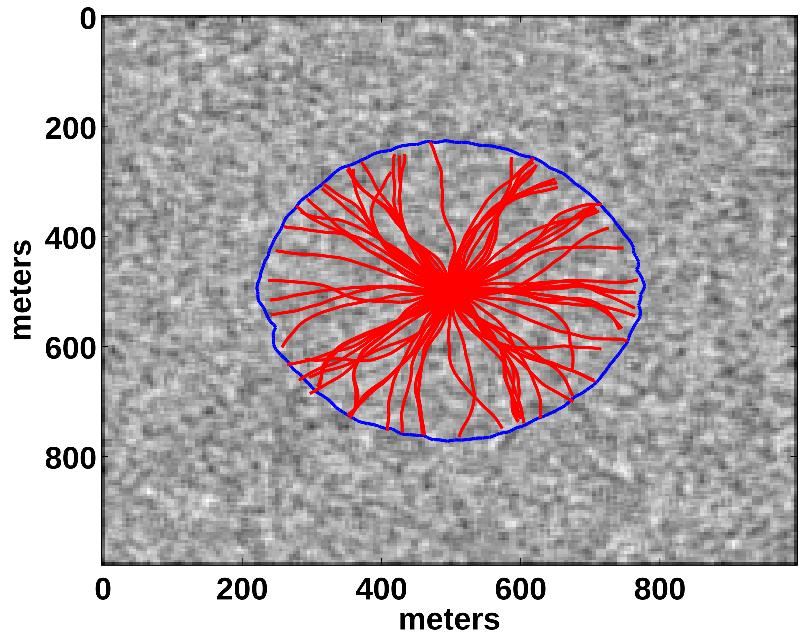

FIG. 2. Ray tracing (in red) through a $2000m/s, \sigma = 500m/s$ medium with light smoothing. The eikonal solution envelope for the same propagation time is overlaid in blue.

as in Figure 2. With heavy smoothing, the match is even better (Figure 3). This, however, raises the question, is this *better physics*?

In a velocity model with extreme random variation, a finite-difference solution as shown in Figure 4 does reveal a wavefront in the expected location. However, a significant portion of the energy of the wavefield is represented by the multiply-scattered waves inside the wavefront. Although the wavefront is distinct, it is not necessarily where the vast majority of the energy may always be found. Physically, then, perhaps the ray-tracing in Figure 1 is an appropriate approximation of the sort of propagation seen in Figure 4 in that the ray path ends proportionally represent the location of the energy of the propagation.

In terms of seismic migration, however, this question is not quite so important. Velocity models for ray-tracing are not usually full of random variations, so we would expect that ray-tracing-derived traveltimes and solutions to the eikonal equation would be a closer match – at least in the case of simple out-going wavefields. Therefore, we will treat the eikonal solution as as limiting case of ray-tracing, valid when ray-tracing through media free from extensive local variability.

FREQUENCY-DEPENDENT SMOOTHING OF A BANDED VELOCITY MODEL

Since frequency-dependent smoothing of the velocity model was shown to be effective in improving imaging via GPSPI (Hogan and Margrave, 2006), it is natural to wonder whether ray-tracing and/or eikonal solutions may benefit from this as well.

To test this, we generated a velocity model consisting of horizontal stripes of alternating high-velocity/low-velocity bands (Figure 5). This original velocity model was smoothed several times with Gaussian smoothers $\sigma = 0 – 25$m. The variously-smoothed velocity

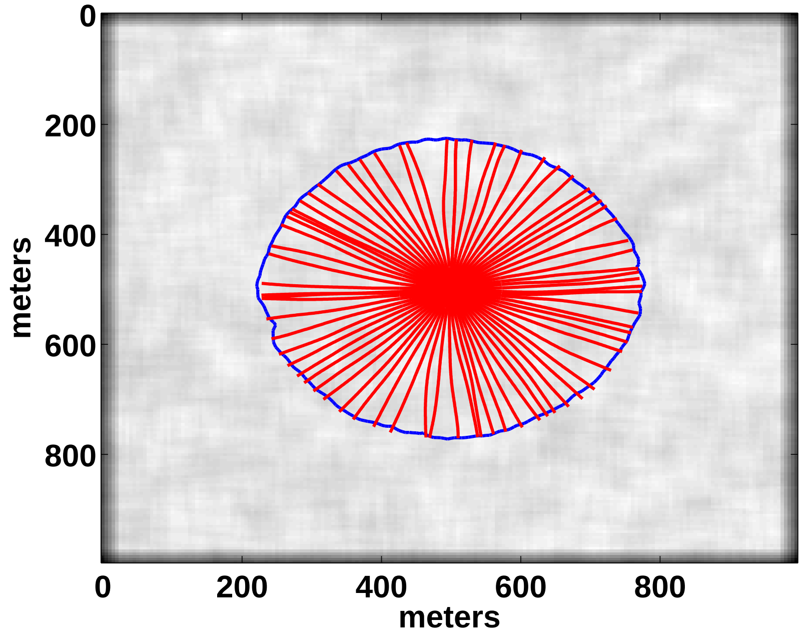

FIG. 3. Ray tracing (in red) through a $2000m/s, \sigma = 500m/s$ medium with heavy smoothing. The eikonal solution envelope for the same propagation time is overlaid in blue.

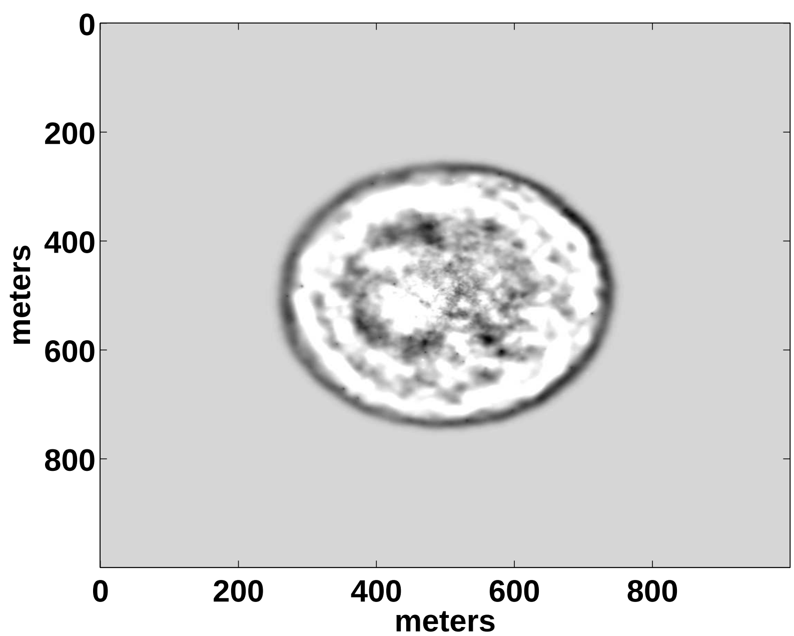

FIG. 4. Finite differences solution of a $2000m/s, \sigma = 200m/s$ medium. A distinct wavefront is visible.

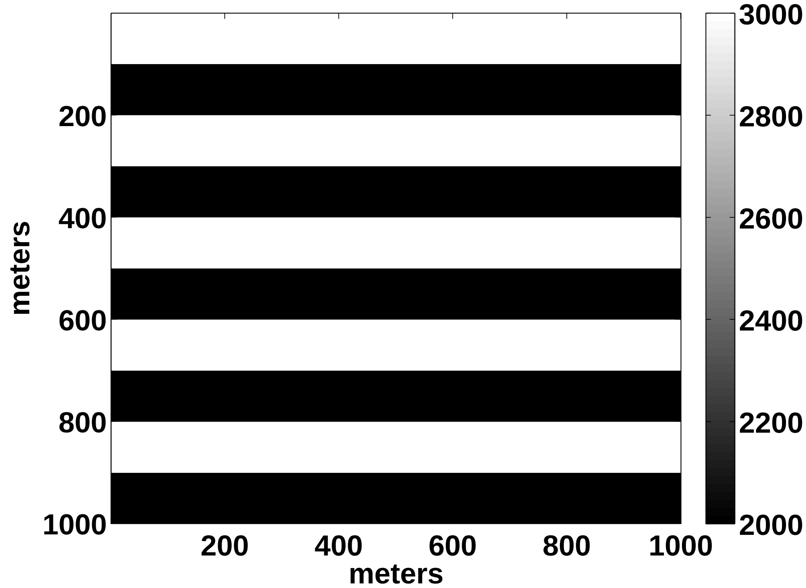

FIG. 5. Striped velocity model, velocity in m/s

models are shown in Figure 6.

A finite-difference solution of the wave equation over this domain with a high-frequency (60 Hz dominant minimum-phase) source at (500,500) was calculated to a final time of $t = 0.136s$, and a solution of the eikonal equation over the same domain was also calculated. These solutions may be seen in Figure 7. The position of the outgoing wavefront may be seen to agree well with the eikonal contour.

Next, lower-frequency finite-difference wavefields were calculated over the same unsmoothed medium. At the extreme low-frequency end (2 Hz dominant minimum phase source), the outermost envelope of the wavefield coincides best with an eikonal solution over the original velocity model smoothed by convolving with a Gaussian smoother with σ=25m, *ie* a smoothing length of 25m. For comparison, Figure 9 shows eikonal solutions for both unsmoothed and smoothed velocity models overlaid on the finite-difference solution with a 2 Hz dominant source. At approximately (500, 800) on Figure 9, it may be seen that the smoothed-model eikonal contour extends farther down in the section than the amplitude of the original wavefield. This may be explained by considering the velocity model in Figure 6. The 25m smoother smears the high-velocity band between 800m and 900m depth up into the low-velocity band between 700m and 800m. Thus the eikonal contour locally out-paces the actual velocity of propagation in this direction. This is purely a local effect, and is corrected upon farther propagation. Similar smoothed-model eikonal solutions are overlaid on finite-difference solutions for a 5 Hz dominant source (Figure 10), 10 Hz dominant source (Figure 11), 20 Hz dominant source (Figure 12), and a 40 Hz dominant source (Figure 13).

Overall results are summarized in Figure 14. At high frequency, the eikonal solutions match the finite difference wavefield well. At lower frequencies, smoothing lengths up to σ =25m become necessary.

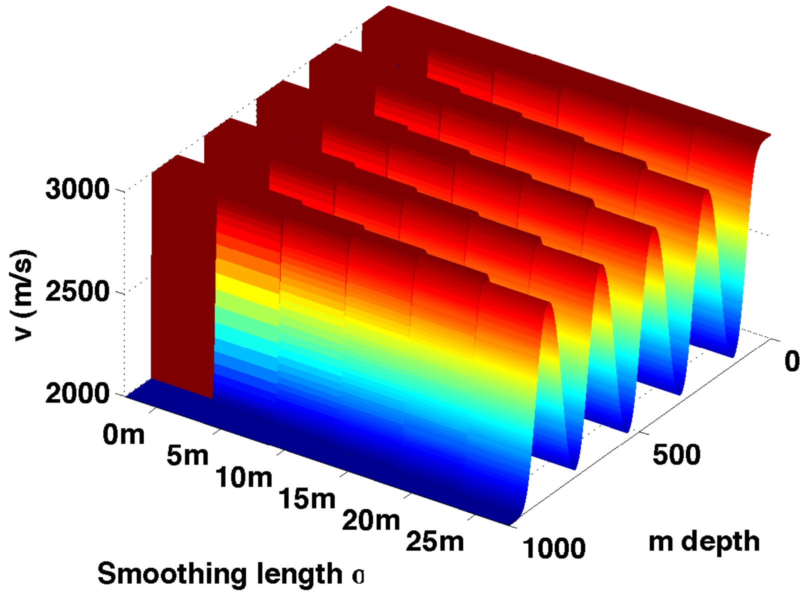

FIG. 6. Vertical sections of the velocity models used for eikonal solutions. On the left is the unsmoothed velocity model, on the right is the most heavily smoothed model.

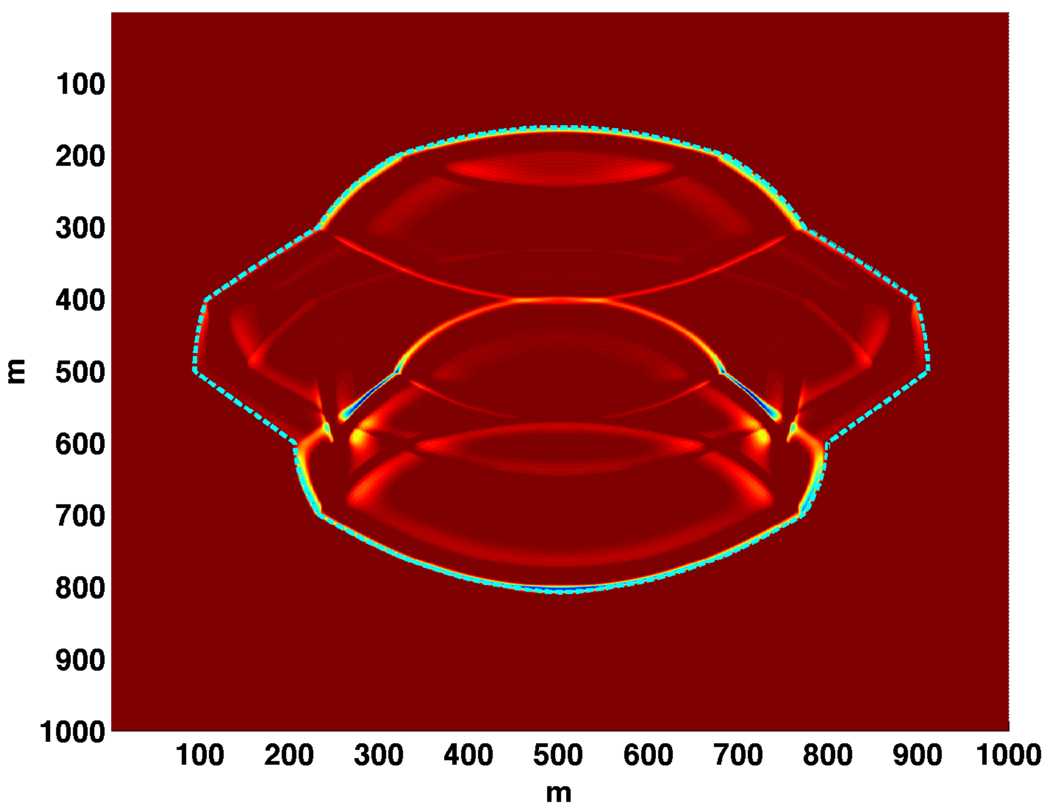

FIG. 7. 60 Hz dominant source in unsmoothed velocity model, with eikonal solution to the unsmoothed model overlaid in blue.

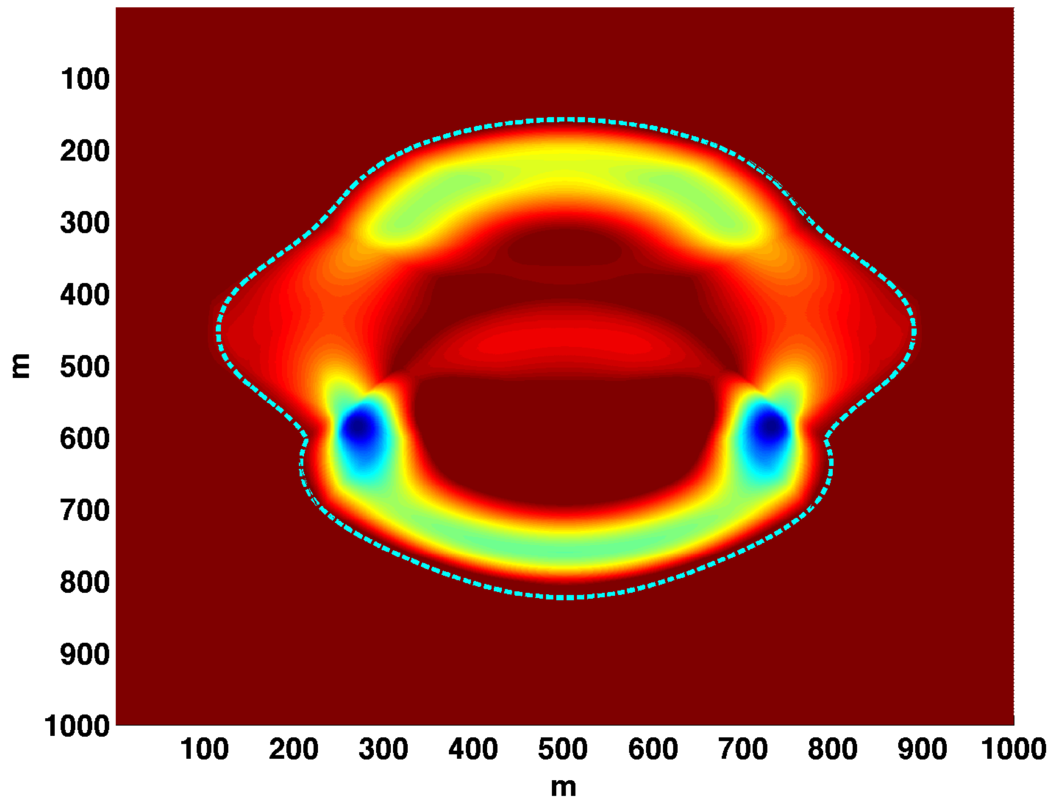

FIG. 8. 2 Hz dominant source, with eikonal solution to the 25 m smoothing length model overlaid in blue.

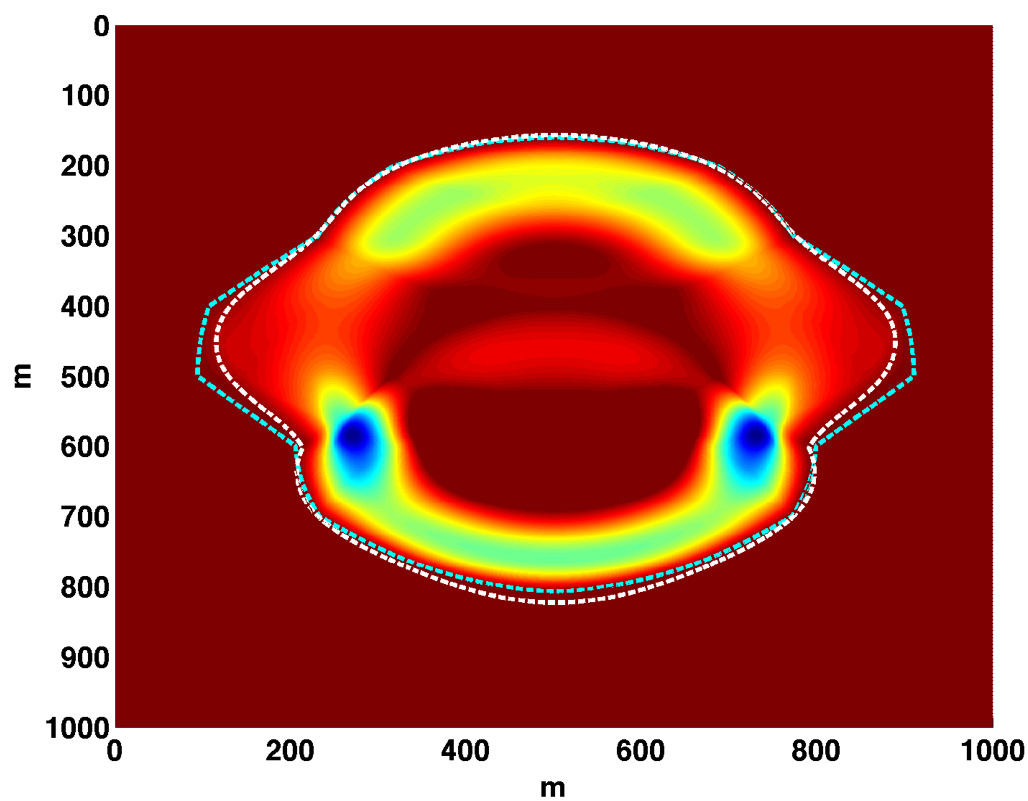

FIG. 9. 2 Hz dominant source, 25 m smoothing length eikonal solution in white, unsmoothed velocity model eikonal solution in blue.

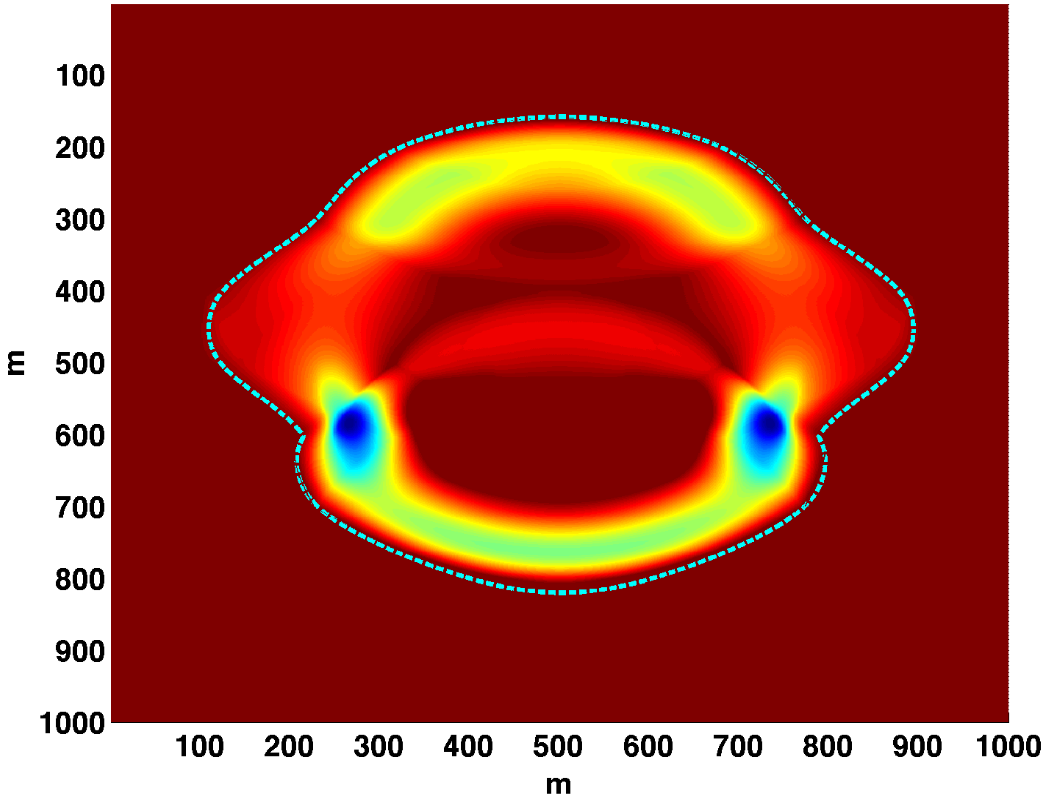

FIG. 10. 5 Hz dominant source, eikonal solution to 20 m smoothing length model overlaid in blue.

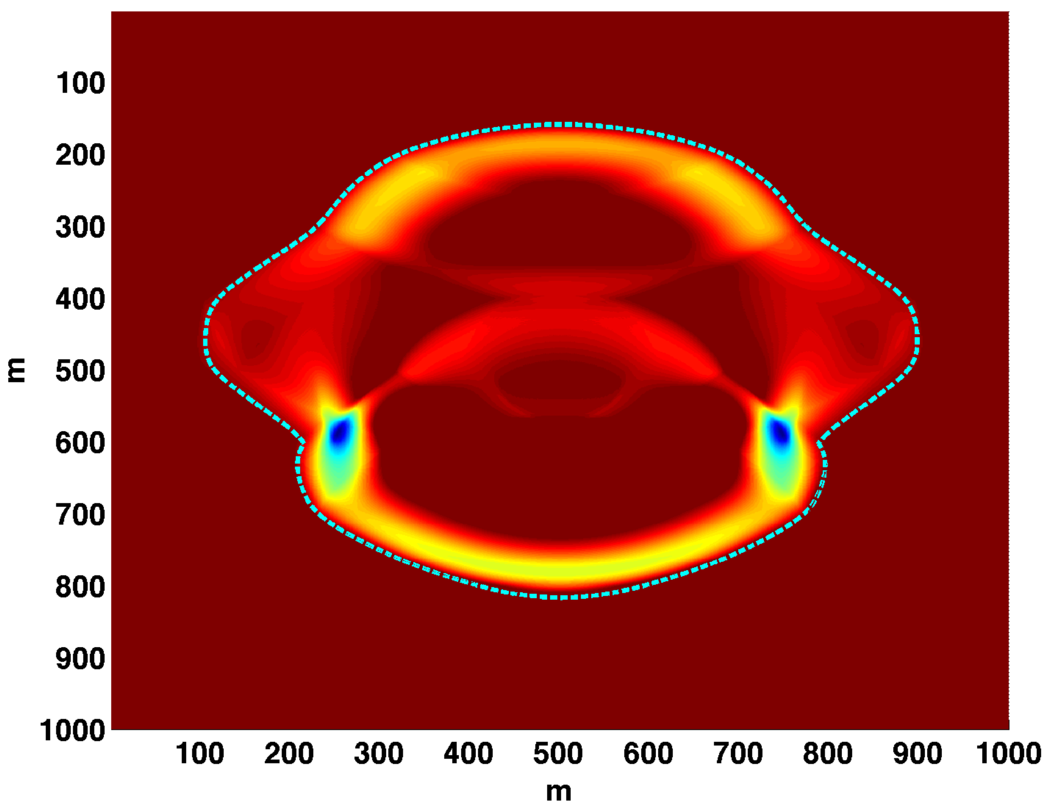

FIG. 11. 10 Hz dominant source, eikonal solution to 15 m smoothing length model overlaid in blue.

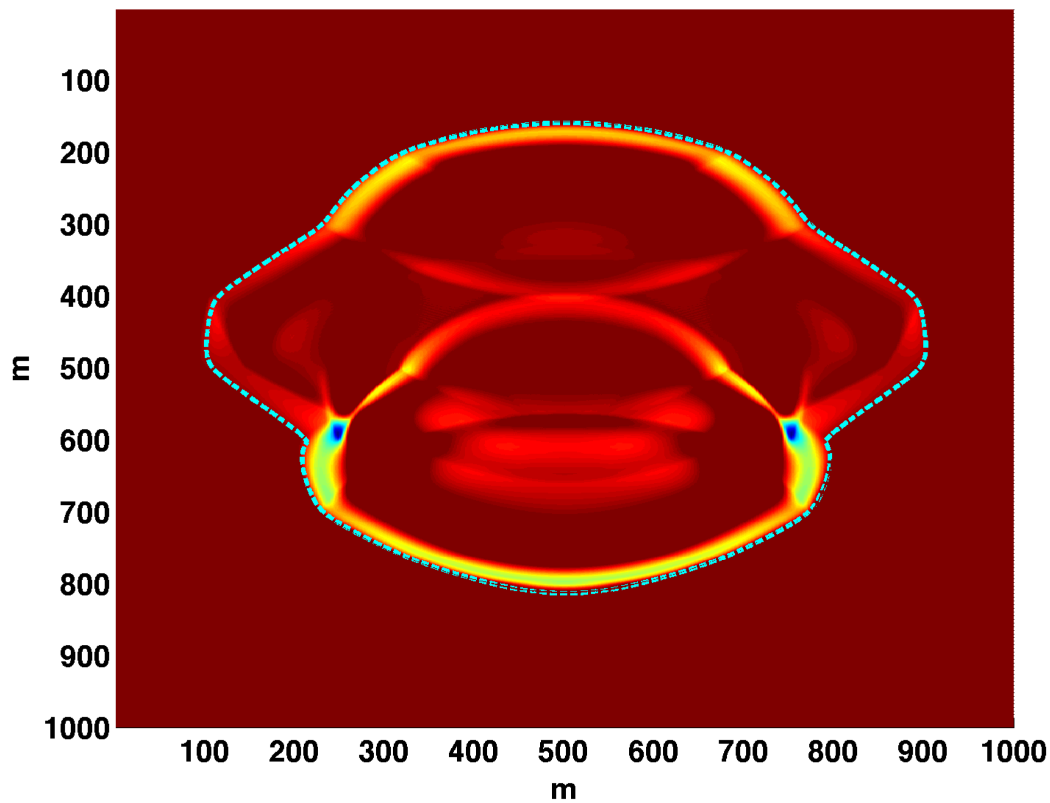

FIG. 12. 20 Hz dominant source, eikonal solution to 10 m smoothing length model overlaid in blue.

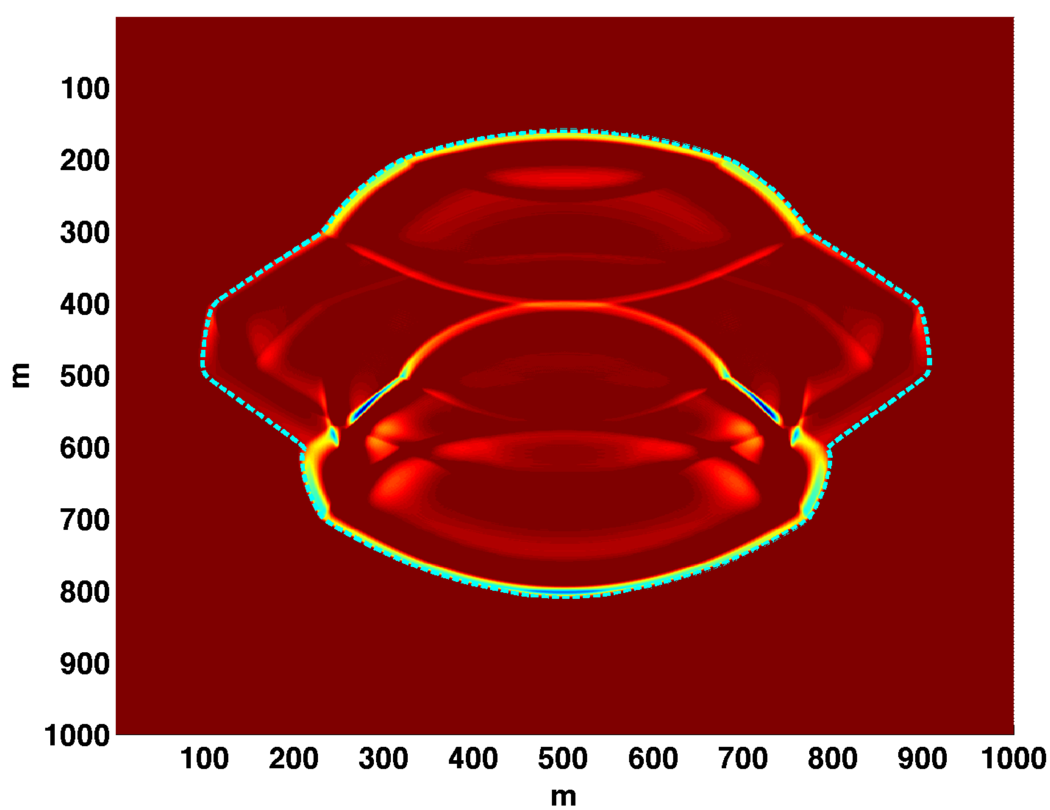

FIG. 13. 40 Hz dominant source, eikonal solution to 5 m smoothing length model overlaid in blue.

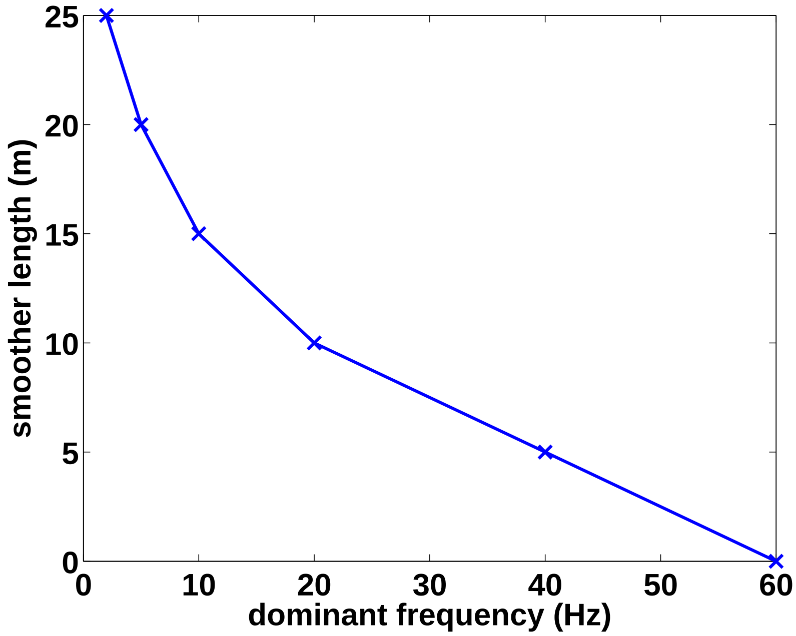

FIG. 14. Smoothing length as a function of dominant frequency.

EFFECTS OF SMOOTHING ON RAY-TRACING

Figure 15 shows the result of tracing rays through the unsmoothed medium. Many of the rays terminate on the eikonal contour as expected. However, several rays appear to reflect and terminate inside the contour. This highlights one major difference between eikonal-based modelling and ray-tracing modelling: ray-tracing allows for more natural inclusion of the modelling of multiple reflections, while eikonal solutions are often insensitive to multiple reflections*. Whether or not either is a benefit or hindrance is dependent on the goals of the modelling. When the velocity model is smoothed, ray-tracing and eikonal solutions converge: that is, more rays terminate exactly at the eikonal contour as in Figure 16.

In Figure 17, the 60 Hz source wavefield is shown with rays traced. Here it is clear that the reflected rays are following the high-amplitude reflected event in the full wavefield. By contrast, in Figure 18, the smoothed velocity model allows the raypaths to accurately track the envelope of the low-frequency wavefield.

CONCLUSIONS AND FUTURE WORK

Frequency-dependent smoothing of a velocity model can lead to eikonal and ray-tracing solutions which match the propagation envelope of a full wavefield better at low frequencies, where these approximations are not strictly valid. At these lower frequencies, the smoothed velocity model also leads to ray-tracing solutions which converge to give the same kinematics as the eikonal solutions.

*though this can depend on the actual algorithm employed to solve the eikonal equation.

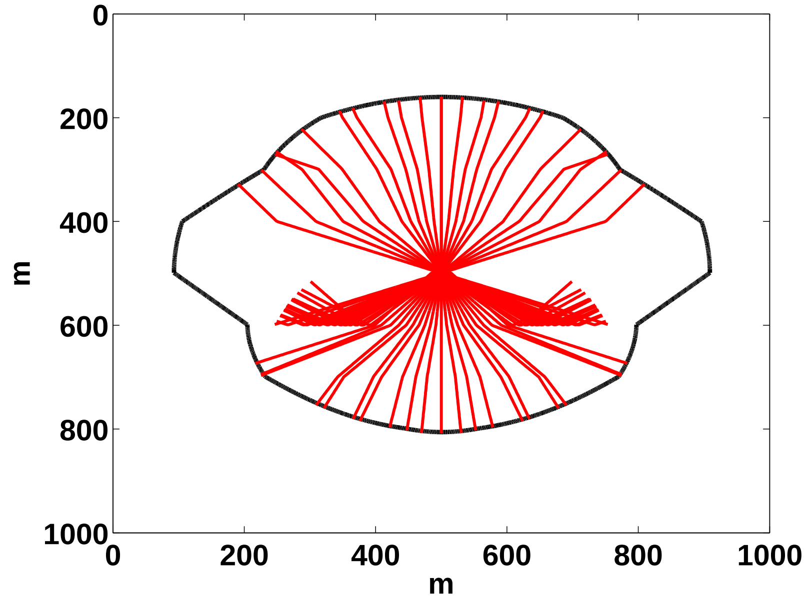

FIG. 15. Ray-tracing through the unsmoothed velocity model, with eikonal contour.

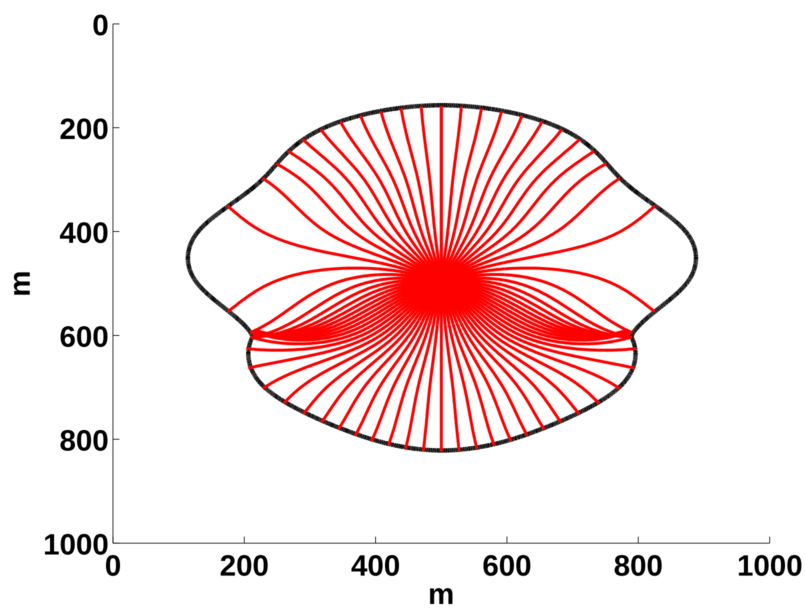

FIG. 16. Ray-tracing through the 25m smoothed velocity model, with eikonal contour.

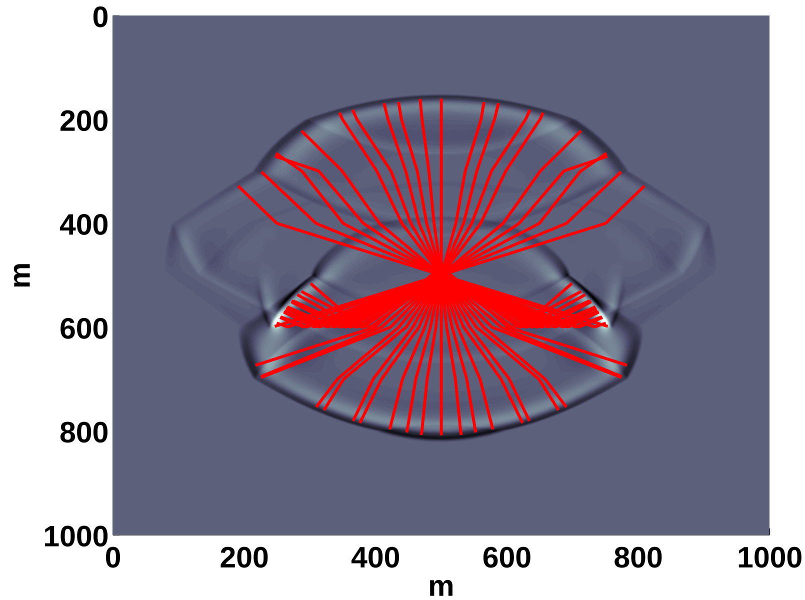

FIG. 17. Ray-tracing through the unsmoothed velocity model, with 60 Hz dominant finite difference wavefield.

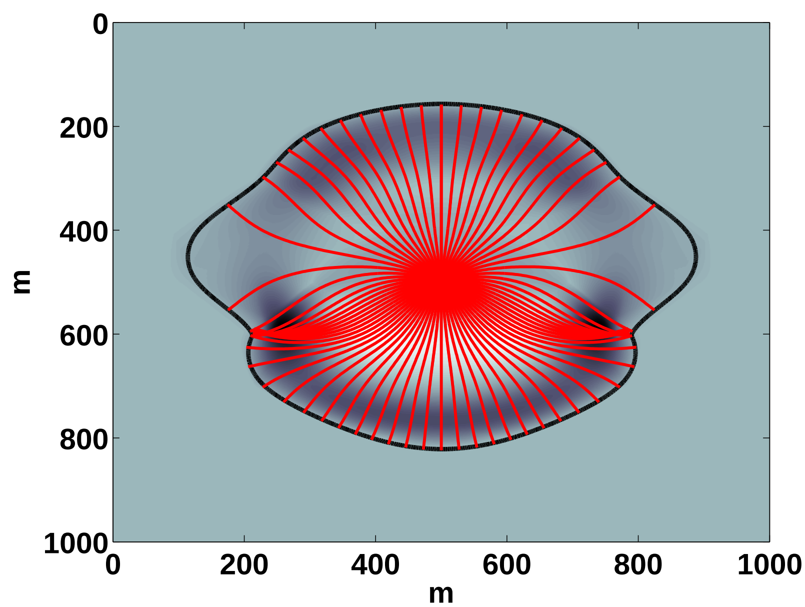

FIG. 18. Ray-tracing through the 25m smoothed velocity model, with 2 Hz dominant finite difference wavefield.

In the future, we will continue to investigate the full behaviour of these high-frequency approximations at low frequencies. We are currently working towards analytical approaches to determine optimal smoothing length. Additionally, we are considering alternative scale-dependent representations of given velocity models that may be more effective than a simple frequency-dependent smoothing. Specifically, we are looking at extensive linearizations of the hypereikonal equation that may allow for simple but theoretically-justifiable frequency-dependent velocity models.

REFERENCES

Biondi, B., 1997, Solving the frequency-dependent eikonal equation, Tech. Rep. 73, Stanford Exploration Project.

Hogan, C. M., and Margrave, G. F., 2006, Frequency-dependent velocity smoothing in GPSPI migration, Tech. rep., CREWES Research Report.

Margrave, G. F., and Ferguson, R. J., 1999, Wavefield extrapolation by nonstationary phase shift: Geophysics, **64**, 1067–1078.

Pujol, J., 2003, Elastic wave propagation and generation in seismology: Cambridge University Press.

Woodward, M. J., 1992, Wave-equation tomography: Geophysics, **57**, No. 1, 15–26.